Application of Leading-Edge Vortex Manipulations to Reduce Wing Rock Amplitudes

James Walton* and Joseph Katz†
San Diego State University,
San Diego, California 92182

Introduction

THE extension of an airplane's performance envelope into the high angle-of-attack region to improve maneuverability often carries the penalty of undesirable instabilities. One frequently encountered lateral instability is the limit-cycle roll oscillation, "wing rock," which is driven by strong, concentrated vortices originating from the leading edges of highly swept lifting surfaces.[1-8] Mathematical models[9-17] at various levels of complexity have clarified the role of these vortices in driving the rolling motion. Simultaneously accumulated experimental evidence[18,19] indicates that a wing's rolling moment can be affected by mechanical or pneumatic manipulation of these vortices. Since these vortices generate the much needed high-lift coefficients at larger angles of attack, it is logical to assume that control of this undesirable roll oscillation is possible by manipulating the strength and/or location of the vortices[18-20] that cause the wing rock.

In the present study, a simple flap system was incorporated into the front section of a slender double-delta wing where the leading-edge vortex motion could be influenced by moving these flaps (Fig. 1). Since analytical studies[21] on the control of wing rock indicate that a feedback of the roll oscillation rate, or a frequency shift between the wing motion and the control device, can generate damping of the motion, the proposed flap system was activated (mechanically) at the same frequency of the rolling motion. Also, instead of feeding back the roll rate, a relative phase shift (between the oscillatory motions of the flaps and wing) was imposed due to the mechanical simplicity required for such a wind-tunnel model.

Experimental Apparatus

A schematic description of the "free-to-roll" wind-tunnel model is shown in Fig. 1 (top) and additional geometrical details of the model are provided in the bottom of Fig. 1. Each leading-edge flap was mounted on two roller bearings to reduce friction, and the size of these bearings dictated the wing thickness. Intuitively, the flaps should have been placed at the most forward position, starting at the apex, but because of the large size of the bearings the flaps were moved approximately 45% of the chord behind the appex. Consequently, to increase the likelihood of being able to manipulate leading-edge vortex location by such simple leading-edge flap deflections, a double-delta wing shape was used. This choice is based on experimental evidence[22-24] indicating that a second vortex forms near the leading-edge break point and, therefore, the flaps were placed behind this point. (As most high-speed airplanes have thin, highly swept strakes that cannot house movable control surfaces, the above placing permits the flaps to be placed in the thicker wing section of an actual airplane, just behind the strakes.)

The mounting of the model in the test section was similar to that used in most free-to-roll experiments.[1-3,7] The potentiometer for measuring the angular position and the bearings were mounted inside a central cylinder, as shown in Fig. 1. Friction due to the bearings and flap actuating mechanism was small compared to the aerodynamic moments and it was on the order of 0.1 N·cm [which is less than C_l = Moment/$(\frac{1}{2}\rho V_\infty^2 Sb) \approx 0.001$, at V_∞ = 36 m/s].

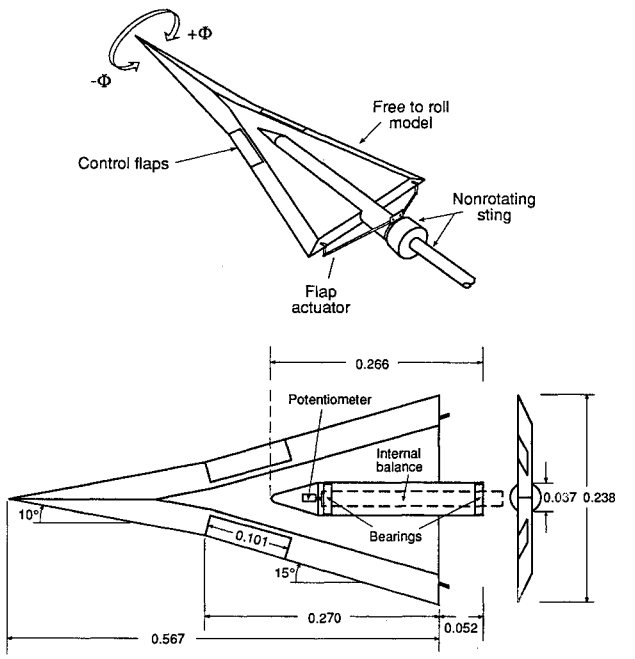

Fig. 1 Three-quarter view of the wing-rock model and its principal dimensions (dimensions in mm).

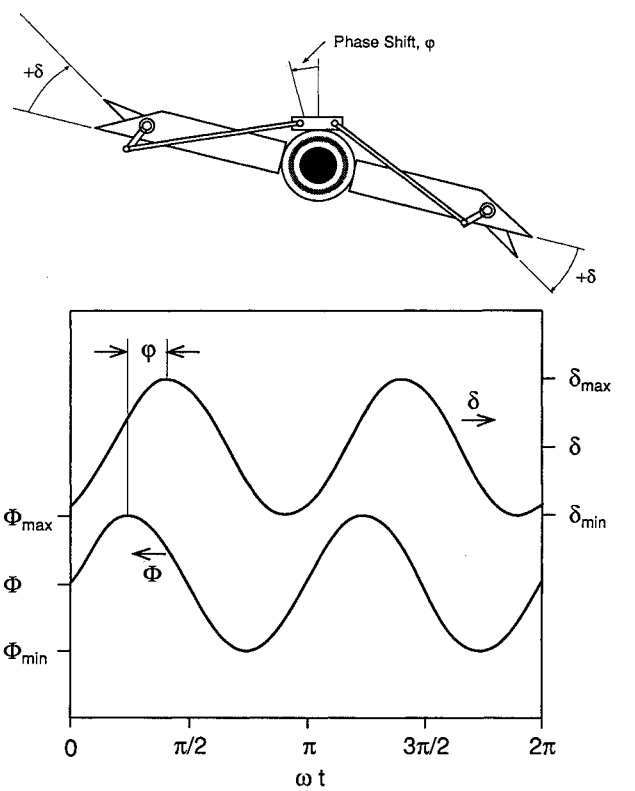

Fig. 2 Definition of the phase shift (φ) between wing roll angle Φ, and flaps deflection δ. The mechanical flap-actuating linkages are shown schematically on the upper part of the figure.

Presented as Paper 92-0279 at the AIAA 30th Aerospace Sciences Meeting and Exhibit, Reno, NV, Jan. 6–9, 1992; received June 12, 1992; revision received Sept. 2, 1992; accepted for publication Sept. 3, 1992.

*Graduate Student, Department of Aerospace Engineering. Member AIAA.

†Professor, Department of Aerospace Engineering. Associate Fellow AIAA.

The wind tunnel (closed-return type) has an inlet contraction ratio of 1:7 and has test-section dimensions of 0.81-m high and 1.15-m wide. Model to test section frontal-area cross section ratio was less than 3% for $\alpha = 45$ deg, and therefore, no wind-tunnel blockage corrections were applied to the data. (Ref. 25 suggests 7.5% as the maximum allowable blockage.) Test speeds varied between 17–36 m/s, corresponding to $Re_c \approx 0.11 \times 10^6$ to 0.23×10^6, where the Reynolds number is based on the wing's chord. Since the model's leading edges were sharp (Fig. 1), it is believed that the effect of Reynolds number is relatively small, and therefore, the results of this test can be considered to be relevant to larger Reynolds numbers.

The mechanical actuators and the two rods were connected to an external cylinder (which did not rotate with the wing) and are shown schematically in the upper portion of Fig. 2. This external cylinder allowed adjustment of the phase shift (by changing the angular position of the external cylinder) between the wing and the flaps' oscillatory motions. The phase shift φ between the oscillatory motions of the two flaps and the wing is defined in the lower part of Fig. 2; e.g., if $\varphi = 0$ the maximum flap deflection δ_{max} is reached at the maximum roll angle Φ_{max}. Through the mechanical flap actuators (shown in Fig. 2), the flap amplitude δ_{max} depended on the roll angle amplitude Φ_{max} and the phase shift φ. Positive flap deflection (for the right side) was measured in the direction of the rolling angle (shown in Fig. 1, top); thus, Fig. 2 depicts the positive deflection for both flaps (e.g., right flap down and left flap up). Note that the flap angle variation was close to, but was not a pure sinusoidal oscillation because of the simple linkage geometry (shown in Fig. 2).

Experimental Results

The double-delta wing model with locked flaps (at $\delta = 0$ deg, flush with the wing) did exhibit self-induced roll oscillations within the angle of attack range of 20 deg $< \alpha <$ 45 deg. During these experiments all flap actuating linkages were connected so that the damping effect due to mechanical friction (when comparing with the moving flap case) would be minimized. Then for the roll damping experiments a flap angle δ and a phase shift φ could be selected by adjusting the length or position of the control rods (see Fig. 2) until a significant reduction in the roll angle amplitude was observed. These observations indicated that with the present flap system the most effective damping (judging by the reduction in roll amplitude) was obtained when the flap motion was in phase ($\varphi \approx 0$ deg) or in antiphase ($\varphi \approx 180$ deg). Consequently, the investigation was centered around these phase shift values.

To demonstrate the effect of the flap system on the free-to-roll oscillations, the roll angle history with and without activating the flaps is presented in Fig. 3. The largest roll angle amplitude for the wing without the flaps was observed at about $\alpha = 25$ deg, and when activating the flaps, the largest reduction in these roll angle amplitudes was obtained at a phase shift of $\varphi = 15$ deg. Therefore, the data presented in Fig. 3 represent the most effective rolling moment amplitude reduction observed throughout this experiment.

The roll angle variation for the basic wing with fixed flaps (nonmoving at $\delta = 0$ deg) is shown at the left side of Fig. 3. By oscillating the flaps at the same frequency of the roll oscillations, with an amplitude of $\delta_{max} = 15$ deg, the roll-angle amplitude was reduced considerably. Over an extended time period the wing showed limited bursts of roll oscillations, as shown in the center of Fig. 3, possibly due to flow disturbances (after which the rolling motion would almost stop until the next flow disturbance would initiate another such perturbation).

Limited flow visualization (mainly with tufts) indicated that because of the thick wing and the large bevel angle of the wing leading edge, the flap vortex was interacting in a complex manner with vortices originating at the leading-edge sections ahead of and behind the flap and with those originating at the gap caused by the flap deflection. In an effort to achieve a simpler vortex structure, the wing was inverted so that mainly two dominant leading-edge vortices (per side) will be present, and the flap amplitude was reduced to $\delta_{max} = 10$ deg. The results for this case are presented at the right side of Fig. 3 showing that the roll-oscillation amplitude became even smaller (note that for the inverted wing, with $\delta = 0$, the oscillation amplitude levels were lower than those presented at the left side of Fig. 3, and for this case $\Phi_{max} \approx 15$ deg).

The achieved reduction of the self-induced oscillation amplitude with the present wing/flap system is summarized in Fig. 4. The dashed horizontal line depicts the oscillation amplitude observed with flaps taped to the wing at $\delta = 0$ deg (see left side of Fig. 3). The oscillation amplitudes for the "flaps-up" case (explained in the next paragraph) were very close to the value obtained with the flaps at $\delta = 0$ deg, shown by the dashed line, whereas for the inverted wing case, Φ_{max} was $\approx$15 deg as noted before. In general, the best amplitude reductions were obtained with a phase shift of $\varphi = -15$ deg or $\varphi = 180 - 15$ deg $= 165$ deg, but other ranges of sizable amplitude reduction are visible. For the larger angles of attack[27] the relative amplitude reduction is smaller due to the initially smaller roll angle amplitudes.

The basic approach of this study was to seek a simple method to disturb the leading-edge vortex location by the two movable flaps. The large wing thickness and leading-edge bevel seemed to reduce the effectiveness of the flaps, and therefore, the two flaps were raised by 20 deg into the flow (such that at $\Phi = 0$ and $\varphi = 0$, $\delta = 20$ deg at the left side and $\delta = -20$ deg at the right side) so that they will be closer to the vortex originating at the apex. This case was somewhat more effec-

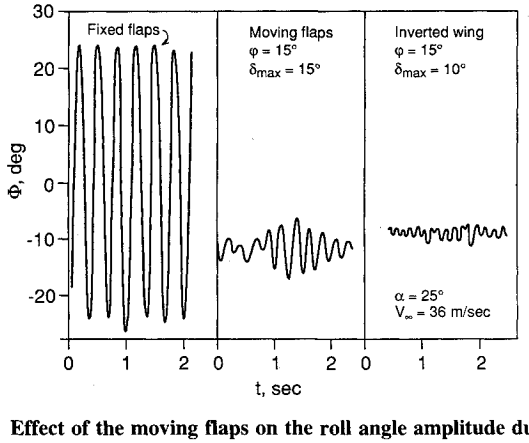

Fig. 3 Effect of the moving flaps on the roll angle amplitude during the self-induced oscillations.

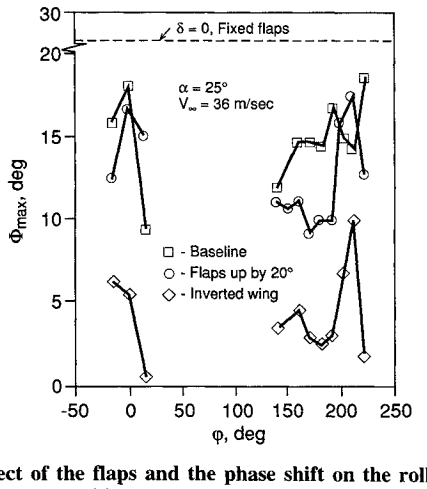

Fig. 4 Effect of the flaps and the phase shift on the roll angle amplitude during the self-induced oscillations.

tive in reducing the oscillation amplitudes and the corresponding results are represented by the circles in Fig. 4.

The inverted wing with the planar upper surface presents a case where the flaps' leading edge is closer to the vortices originating from the leading-edge portion ahead of the flaps. Consequently, for this configuration, smaller oscillation amplitudes are expected (indeed, as shown by the diamond symbols in Fig. 4) due to the larger effect of the flap motion.

Acknowledgment

This work was supported by NASA Ames Research Center, under Grant NCC-2-458, with James Ross as project monitor.

References

[1]Nguyen, L. T., Yip, L., and Chambers, J. R., "Self Induced Wing Rock of Slender Delta Wings," AIAA Paper 81-1883, Aug. 1981.

[2]Levin, D., and Katz, J., "Dynamic Load Measurements with Delta Wings Undergoing Self-Induced Roll Oscillations," *Journal of Aircraft*, Vol. 21, Jan. 1984, pp. 30–36.

[3]Katz, J., and Levin, D., "Self-Induced Roll-Oscillations Measured on a Delta Wing/Canard Configuration," *Journal of Aircraft*, Vol. 23, Nov. 1986, pp. 801–807.

[4]Jun, Y. W., and Nelson, R. C., "Leading Edge Vortex Dynamics on a Slender Oscillating Wing," *Journal of Aircraft*, Vol. 25, Sept. 1988, pp. 815–819.

[5]Ng, T. T., Malcolm, G. N., and Lewis, L. C., "Flow Visualization Study of Delta Wing in Wing-Rock Motion," AIAA Paper 89-2187, Aug. 1989.

[6]Arena, A. S., and Nelson, R. C., "The Effect of Asymmetric Vortex Wake Characteristics on a Slender Delta Wing Undergoing Wing Rock Motion," AIAA Paper 89-3348, Aug. 1989.

[7]Levin, D., and Katz, J., "Self-Induced Roll Oscillations of Low-Aspect Ratio Rectangular Wings," AIAA Paper 90-2811, Aug. 1990.

[8]Arena, A. S., and Nelson, R. C., "Unsteady Surface Pressure Measurements on a Slender Delta Wing Undergoing Limit Cycle Wing Rock," AIAA Paper 91-0434, Jan. 1991.

[9]Konstadinopoulos, P., Mook, D. T., and Nayfeh, A. H., "Numerical Simulation of the Subsonic Wing Rock Phenomenon," AIAA Paper 83-2115, Aug. 1983.

[10]Ericsson, L. E., "The Fluid Mechanics of Slender Wing Rock," *Journal of Aircraft*, Vol. 21, May 1984, pp. 322–328.

[11]Konstadinopoulos, P., Mook, D. T., and Nayfeh, A. H., "Subsonic Wing Rock of Slender Delta Wings," *Journal of Aircraft*, Vol. 22, No. 3, 1985, pp. 223–228.

[12]Ericsson, L. E., "Analytic Prediction of the Maximum Amplitude of Slender Wing Rock," *Journal of Aircraft*, Vol. 26, No. 1, 1989, pp. 35–39.

[13]Hsu, C. H., and Lan, C. E., "Theory of Wing Rock," *Journal of Aircraft*, Vol. 22, No. 10, 1985, pp. 920–924.

[14]Elzebda, J. M., Mook, D. T., and Nayfeh, A. H., "Influence of Pitching Motion on Subsonic Wing Rock of Slender Delta Wings," *Journal of Aircraft*, Vol. 26, No. 6, 1989, pp. 503–508.

[15]Elzebda, J. M., Nayfeh, A. H., and Mook, D. T., "Development of an Analytical Model of Wing Rock for Slender Delta Wings," *Journal of Aircraft*, Vol. 26, No. 8, 1989, pp. 737–743.

[16]Lee, E. M., and Batina, J. T., "Conical Euler Simulation of Wing Rock for a Delta Wing Planform," *Journal of Aircraft*, Vol. 28, No. 1, 1991, pp. 94–96.

[17]Ericsson, L. E., "Slender Wing Rock Revisited," AIAA Paper 91-0417, Jan. 1991.

[18]Malcolm, G. N., Ng, T. T., Lewis, L., and Murri, D. G., "Development of Non-Conventional Control Methods for High Angle of Attack Flight Using Vortex Manipulation," AIAA Paper 89-2192, July 1989.

[19]Rao, D. M., and Puram, C. K., "Chine Forebody Vortex Manipulation by Mechanical and Pneumatic Techniques on a Delta Wing Configuration," AIAA Paper 91-1812, June 1991.

[20]Ng, T., Ong, L., Suarez, C., and Malcolm, G., "Wing Rock Suppression Using Forebody Vortex Control," AIAA Paper 91-3227, Sept. 1991.

[21]Luo, J., and Lan, E., "Control of Wing-Rock Motion of Slender Delta Wings," AIAA Paper 91-2886, Aug. 1991.

[22]Verhaagen, N. G., "An Experimental Investigation of the Vortex Flow over Delta and Double-Delta Wings at Low Speed," Aerodynamics of Vortical Type Flows in Three Dimensions, AGARD CP-342, Paper 7, Rotterdam, The Netherlands, April 1983.

[23]Erickson, G. E., "Water Tunnel Flow Visualization: Insight into Complex Three-Dimensional Flowfields," *Journal of Aircraft*, Vol. 17, No. 9, 1980, pp. 656–662.

[24]Hoejimakers, H. W. M., Vaatsra, W., and Verhaagen, N. G., "Vortex Flow over Delta and Double-Delta Wings," *Journal of Aircraft*, Vol. 20, No. 9, 1983, pp. 825–832.

[25]Rae, W. H., Jr., and Pope, A., "Low-Speed Wind Tunnel Testing," Wiley, New York, 1984, p. 371.

[26]Morris, S. L., and Ward, D. T., "A Video-Based Experimental Investigation of Wing Rock," AIAA Paper 89-3349, Boston, MA, Aug. 1989.

[27]Walton, J., and Katz, J., "Reduction of Wing Rock Amplitudes Using Leading-Edge Vortex Manipulations," AIAA Paper 92-0279, Reno, NV, Jan. 1992.

Effects of Wing-Tip Vortex Flaps

Lance W. Traub* and Alan Nurick†
University of the Witwatersrand, Johannesburg, South Africa

Nomenclature

AR	=	aspect ratio, b^2/S
b	=	wing span
C_D	=	drag coefficient, drag/qS
C_L	=	lift coefficient, lift/qS
C_{L_α}	=	lift curve slope
C_M	=	pitching moment coefficient, moment/qSc
c	=	reference chord
e	=	Oswald efficiency factor
q	=	dynamic pressure of freestream
S	=	projected planform area
α	=	angle of attack
δ_F	=	wing tip vortex flap angle

Subscripts

cdmin	=	lift coefficient at which minimum drag occurs
min	=	minimum drag coefficient
0	=	zero lift

Introduction

THE trailing vortex system of a finite lifting wing induces a downwash, and as a consequence a rotation of the freestream velocity vector giving rise to vortex drag.

The importance of wing tip geometry in the generation of vortex drag has propagated several tip-mounted drag reducing devices aimed at improving wing efficiency. Successful concepts include winglets[1–3] and tip sails.[4,5]

Recently, the planar sheared tip has received attention, and its most extreme application (the planar crescent wing) is attributed with a theoretical efficiency exceeding that of a wing with elliptic loading.[6] Vijgen et al.[7] reported in an investigation of sheared tip aerodynamics, an increase in both $(L/D)_{max}$ and aerodynamic efficiency for sheared wings over a comparative basic wing. Naik et al.[8] in comparing a high-aspect ratio wing with a rectangular, elliptic, and a sheared tip, reported the lowest Oswald efficiency factor for the sheared tip. These contradictory results suggest that the performance of sheared tips has not been fully characterized. The drag

Received July 13, 1992; revision received Sept. 15, 1992; accepted for publication Sept. 15, 1992.

*Graduate Student, 1 Jan Smuts Ave., P.O. Wits, 2050.

†Professor, Branch of Aeronautical Engineering, 1 Jan Smuts Ave., P.O. Wits, 2050.